Study of single-star turbulence profilers

A.A. Tokovinin

May 24, 1998

1 Introduction

Remote sensing and measurement of atmospheric turbulence is nowadays a rapidly developing activity which is driven by the needs of adaptive optics, interferometry and astronomical site testing. The classical seeing monitors provide a measure of seeing quality resulting from the integrated effect of all atmospheric layers. This is not enough, however, and we want to know the altitude distribution of turbulence strength, i.e. the C_n^2 profile. In this report a particular class of C_n^2 profilers that use single stars as light source is discussed.

The most known method of optical C_n^2 profile measurements is called SCIDAR [21, 22]. It consists in spatio-angular analysis of the atmospheric speckle pattern at the telescope pupil plane. A suitable double star must be used as a light source. Recently the *generalized SCIDAR* concept was proposed which enables to measure the low-altitude turbulence to which the classical SCIDAR is insensitive [1, 6, 9]. Analysis of this technique in terms of precision and system parameters was made in our previous report [19]. A rather large telescope (of at least 1.2 m diameter) and a very good and fast light detector are needed to realize a profile monitor.

An alternative, more simple profile monitor can be constructed with a small telescope and a single star as a light source. The idea is to analyze the spatial structure of the atmospheric speckle and to reconstruct the profile by a suitable inversion procedure. Such a device called *scintillometer* was built more than 20 years ago and apparently has served for regular profile monitoring [12, 10]. We further discuss this instrument in Sect. 3. Then we propose to implement the same principle using a modern technology (CCD detector with fast on-line signal processing). The theory of the modern scintillometer, its noise and resolution parameters are discussed in Sect. 5.

In some applications the turbulence profile is used to calculate the parameters of interest, e.g. the *isoplanatic angle* θ_0 [7]. It can be measured directly from the intensity fluctuations in a telescope with a suitably shaped aperture, as shown in [11, 17, 10], and this technique is more direct and more accurate than the computations from a profile. We briefly recall the isoplanometer theory in Sect. 4.

In Sect. 6 a review of alternative approaches to turbulence profile measurement is given without detailed analysis of these techniques. Finally, in Sect. 7 the conclusions are given.

2 Theory of scintillation

The turbulence profile in the atmosphere $C_n^2(h)$ must be obtained from the measurements of the spatial structure of scintillation pattern. The measured quantity is the normalized scintillation spatial covariance function $C(\vec{r})$

$$C(\vec{r}) =< \Delta I(\vec{x}+\vec{r})\Delta I(\vec{x}) > / < I >^2 \tag{1}$$

where $I(\vec{x})$ is the stellar intensity distribution in the pupil plane, smoothed by a convolution with finite detector pixels. Angular brackets denote ensemble average. We assume that turbulence is isotropic, so $C(\vec{r})$ depends only on $r = |\vec{r}|$ (has rotational symmetry), and the mean intensity $< I >$ is independent of $\vec{x}$. By definition the *scintillation index* is equal to the normalized intensity fluctuations, i.e. $\sigma_I^2 = C(0)$. The usual theory is valid only for unsaturated scintillations $\sigma_I^2 << 1$ (practically $\sigma_I^2 \leq 0.3$).

The relation between $C(\vec{r})$ and $C_n^2(h)$ which follows from the wave propagation theory [16, 21, 22, 17, 9] is given by

$$C(r) = \int_0^\infty \mathrm{d}h C_n^2(h) Q(r,h), \tag{2}$$

$$Q(r,h) = 0.033 \cdot 16\pi^2 k^2 \int_0^\infty \mathrm{d}f f^{-8/3} \sin^2(f^2 h/2k) J_0(fr) A(f), \tag{3}$$

where $k = 2\pi/\lambda$ is the wave number, f is the modulus of spatial frequency, J_0 is the Bessel function, and $A(f)$ is squared Fourier transform of the detector pixel function, which is assumed to be circular-symmetric for simplicity (for non-circular, e.q. square pixels, the Fourier transform must be averaged over angle). The integration limits in Eq. (3) must in fact be from $1/L_0$ to $1/l_0$, where L_0 and l_0 are turbulence outer and inner scales, respectively. However, the results are practically insensitive to the particular values of these parameters, as demonstrated by Stevens, because the integrand is well-behaved near zero and at infinity.

For a detector with infinitely small pixels we must put $A(f) = 1$. For circular pixels with a diameter D this function has the form

$$A(f) = [2J_1(fD/2)/(fD/2)]^2. \tag{4}$$

Thus, the scintillation index σ_I^2 can be calculated from Eqs.(2, 3) by putting $r = 0$ and using a suitable aperture filter $A(f)$. This will be further exploited in Sect. 4 dealing with isoplanometers.

3 Scintillometer of Ochs et al.

In this instrument [12] the spatial structure of atmospheric speckle in the pupil plane is analyzed by a hardware spatial filter. The filter is a periodic pattern (initially a 1-D grating, then a "checkerboard" 2-D pattern) of reflecting and transmitting areas on a transparent substrate. Reflected and transmitted light fluxes are detected by two photomultipliers. The filter isolates a given spatial frequency, which is made to vary by changing the magnification of the pupil image falling onto the filter. Authors argue that the variance of the difference between transmitted and reflected intensities, normalized by the square of mean intensity, gives a good approximation to the component of the spatial power spectrum of atmospheric speckle pattern at the selected frequency.

The 2-D spatial power spectrum of speckle is proportional to $f^{-11/3}\sin^2(f^2h/2k)$, as can be guessed from Eq.(3) or found in the literature (cf. [10], their Eq. 5). It is an oscillating function of h. Even when finite extent of the spatial filter (limited by telescope aperture size) and the averaging over the spectral band (smearing of the oscillations) are taken into account, the resulting altitude dependence of the filtered scintillation (called the *weighting function*) is different for different filter frequencies. By combining the signal at three spatial frequencies with appropriate weights, Ochs et al. obtain the "composite" weighting functions $W(h)$ which are peaked at selected altitudes and are close to zero at other altitudes. Scintillometer signal is an integral of the product $C_n^2(h)W(h)$ over h.

The altitude resolution of this technique is defined by the width of composite weighting functions. Ochs et al. have chosen 7 composite functions $W_i(z)$, but only 3 or 4 of them are approximately non-overlapping. From Fig. 3 of [12] it can be deduced that the FWHM width of W_1 which peaks at 2.25 km is 3.6 km, and FWHM of W_5 peaking at 10 km is 10 km. So, altitude resolution of the scintillometer $\Delta h/h \approx 1$.

The measurement accuracy of this device can not be estimated, because, as noted by the authors, it is limited by turbulence non-stationarity (the measurements at different spatial frequencies are made sequentially). Non-stationarity effects are partially compensated in data processing, but numerical data on the resulting accuracy of C_n^2 are not given in the original publication. The lowest published values of C_n^2 are below 10^{-18} $m^{-2/3}$ at 15 km, and we may presume that instrument noise must be less than this.

Later it was discovered that the data reduction of scintillometer needs some improvements, namely a more precise filter function and a more accurate spectral response modeling [10]. With these corrections, a good agreement was found between the isoplanatic angles calculated from the scintillometer profiles and measured directly by an isoplanometer. An earlier comparison of isoplanometer and scintillometer was reported in [5], where some scintillometer profiles are also given in Fig. 7. One may note their very smooth character - a consequence of low resolution.

4 Isoplanometers

It is convenient to consider the n-th order *moments* of the turbulence profile $M(n)$ defined as

$$M(n) = \int_0^\infty h^n C_n^2(h)\mathrm{d}h. \tag{5}$$

The seeing (or Fried radius r_0) is directly related to $M(0)$, while the *isoplanatic angle* θ_0 is related to $M(5/3)$ [7, 10]:

$$\theta_0 = [2.905k^2(\sec\gamma)^{8/3}M(5/3)]^{-3/5}, \tag{6}$$

where γ is zenith distance.

It follows from the scintillation theory that scintillation index in a very small telescope ($D << \sqrt{\lambda h}$) is proportional to $M(5/6)$, and scintillation index in a very large telescope ($D >> \sqrt{\lambda h}$) is proportional to $M(2)$. The idea of isoplanometer is to find an intermediate telescope diameter to make the scintillation index approximately proportional to $M(5/3)$. Indeed, as shown by Loos and Hogge [11], a 11 cm telescope gives a rather good approximation to the desired quantity. A still better approximation can be obtained with a double annulus aperture as found by Stevens [17] (see also [10]). Scintillation index in such a telescope is given by Eqs.(2, 3) with $r = 0$ and an aperture factor [10]

$$A(f) = (1-\epsilon_1^2+\epsilon_2^2-\epsilon_3^2)^{-2}\{\frac{2J_1(fD/2)}{fD/2}+\frac{2J_1(\epsilon_2 fD/2)}{\epsilon_2 fD/2}-\frac{2J_1(\epsilon_1 fD/2)}{\epsilon_1 fD/2}-\frac{2J_1(\epsilon_3 fD/2)}{\epsilon_3 fD/2}\}^2, \quad (7)$$

where ϵ_i are the fractional radii of the rings, counting inside out. The isoplanometer uses $D = 20.32$ cm with $\epsilon_1 = 0.369$, $\epsilon_2 = 0.492$ and $\epsilon_3 = 0.689$. If a weighting function $Q(0,h)$ is calculated for this aperture and its ratio to $h^{5/3}$ is plotted against h, a fairly constant value is obtained, except for the altitudes below 1 km. However, it is known that these altitudes contribute very little to $M(5/3)$, and so isoplanometer gives very precise measurements of θ_0.

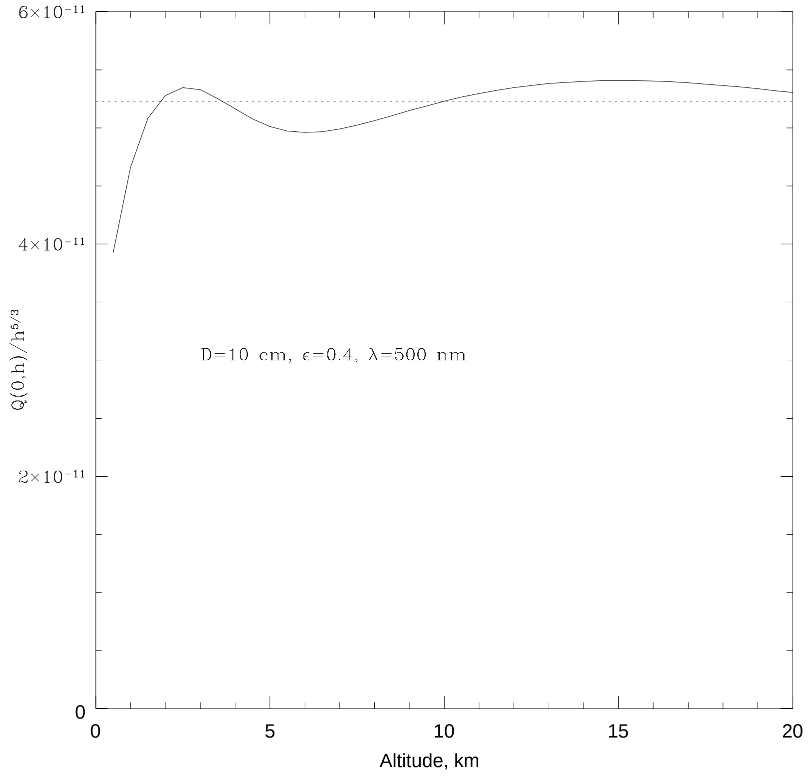

Figure 1: Ratio of the weighting function for scintillation measurements with a 10 cm aperture with 0.4 central obscuration to the ideal $h^{5/3}$ function needed for isoplanatic angle measurement.

In Fig. 1 we plot the ratio $Q(0,h)/h^{5/3}$ for a 10 cm telescope with a central obscuration of $\epsilon = 0.4$, for a wavelength of 500 nm. It can be seen that this aperture provides a good approximation to the desired $h^{5/3}$ weighting - almost as good as a double annulus isoplanometer! When this function is integrated with different realistic turbulence profiles, it is found that errors on θ_0 are well below 5% (R.Conan, private communication). The isoplanatic angle is related to the scintillation index as follows:

$$\theta_0 = B(\sigma_I^2)^{-0.6}, \quad (8)$$

where $B = 0.22''$ for this particular aperture at $\lambda = 500$ nm.

It can be shown that isoplanometer can work on rather faint stars. If photon counts are accumulated with elementary exposure time τ (e.g. $\tau = 10^{-3}$ s) for a total integration time T ($T = 100$ s, for example), the statistical error of photon noise estimate is $N_0^{-1}(T\tau)^{-0.5}$, where

N_0 counts/s is the received flux. If we require that for a typical θ_0 of $2''$ this noise contribution be less than 10% of σ_I^2 (or a 6% accuracy on θ_0), it leads to $N_0 > 1200\ s^{-1}$, or a star brighter than 9th magnitude. The bandpass of 100 nm is assumed here. It is sufficiently narrow to make the atmospheric dispersion effect discussed in Sect. 5.3 negligible for zenith distances less than 30^o. For a given relative measurement accuracy $\epsilon = \sigma_\theta/\theta_0$ the required flux N_0 depends on θ_0:

$$N_0 > 0.6(\theta_0/B)^{5/3}(T\tau)^{-0.5}\epsilon^{-1}. \tag{9}$$

Isoplanometer thus offers an easy and practical way to measure θ_0, its results are more reliable than those of turbulence profilers due to the inherent simplicity of its theory and instrument calibration. Generalizing, we may state that estimates of profile moments $M(n)$ for n from 5/6 to 2 can be obtained from scintillation index measurements with suitably sized and shaped apertures. Extending this approach, we have found a method to estimate $M(0)$ from scintillation measurements with circular and annular apertures, opening way to a new generation of extremely simple and robust seeing monitors [20].

5 Modern scintillometer

With fast CCD detectors and on-line image processing capabilities available now the original concept of Ochs et al. can be substantially improved. Here we investigate an approach which is based on the measurement of intensity correlation function $C(r)$ and subsequent restoration of the profile.

5.1 Theory

Relation between $C(r)$ and $C_n^2(h)$ is given by the Eq.(2), which is to be inverted. When scintillation is observed with a two-dimensional detector, the correlation is determined at a discrete set of baselines $C_i = C(r_i)$. The turbulence profile can also be represented as a combination of M layers at discrete heights h_j (the discretization step in altitude can be made arbitrary small). So, our problem can be re-stated in the matrix form

$$C_i = \sum_{j=1}^{M} Q_{ij} J_j, \tag{10}$$

where $Q_{ij} = Q(r_i, h_j)$. Here i is a baseline index, j - altitude index. The profile $C_n^2(h)$ is replaced by M layers, each layer having the altitude h_j and the integrated turbulence intensity

$$J_j = \int_{\text{layer } j} C_n^2(h)\mathrm{d}h. \tag{11}$$

The matrix Q can be calculated, and Eq.(10) can be formally inverted to obtain the turbulence profile J from the measured correlation C. However, this is a typical inverse problem: the matrix Q is ill-conditioned [1] and the direct inverse solution is so sensitive to the noise in the input data that is it practically useless. The physical reason is that the $C(r)$ produced by a single turbulent layer (or, equivalently, the j-th column of the matrix Q) depends on the layer

[1] The ratio of the largest eigenvalue to the smallest one is called the condition number of a matrix. Large condition numbers mean bad matrices.

altitude in a very smooth manner, so that layers at slightly different altitudes produce almost identical correlation functions $C(r)$.

Still, the layers at significantly different altitudes lead to the measurable difference in the shape of $C(r)$. The key to the solution of our inverse problem lies in reducing the required vertical resolution of the profile. If we try to retrieve only the information that is *really* contained in the input data, the ill-conditioned problem can be solved! Evidently, there is a compromise between resolution and accuracy: the higher is the resolution, the higher is reconstruction noise.

Reducing resolution means smoothing the profile J. Both smoothing and solving the Eq.(10) are linear operations. So, we can limit our study to the *linear* restoration techniques. In this case profile noise would always be proportional to the input noise, the proportionality coefficient depending on the required resolution.

Let us consider an arbitrary set of k linear operators R_k which are applied to the input data vector C_i. The result can be written as

$$S_k = \sum_{i=1}^{N} R_{ki} C_i. \tag{12}$$

Here the matrix R produces the solution vector S. Dimension of this vector can be arbitrary. How shall we choose R to obtain a solution that would approximate the true profile J? The relation between S and J can be obtained by substituting Eq. (10) into (12) and re-arranging the sums:

$$S_k = \sum_{j=1}^{M} W_{kj} J_j, \tag{13}$$

with

$$W_{kj} = \sum_{i=1}^{N} Q_{ij} R_{ki}. \tag{14}$$

Here is the answer: any linear operator R_k corresponds to some *weighting function* W_k, and the action of R_k on input data C gives a result which is equal to the profile "weighted" by W_k. If we want the true (unsmoothed) profile, W_{kj} should be identity matrix, and R_{ki} is the Q^{-1} matrix - i.e. the inverse solution is obtained. For any selected smoothing function W the corresponding operator R can be found by solving Eq.(14) (there is no experimental data in this equation, hence no noise; some subtleties are discussed below, however). We can select as much W-functions as we like and obtain the corresponding matrix R.

The noise in the input data C will enter into the solution S via the operator R. Suppose for simplicity that all N data points C_i have the same additive uncorrelated noise σ (in fact the speckle noise in the ACF is correlated at distances smaller than speckle size). Then it is easy to find the noise of the solution component S_k:

$$\sigma_k^2 = \sum_{i=1}^{N} \sigma^2 R_{ki}^2, \tag{15}$$

or

$$\sigma_k = \sigma f_k, \text{ with } f_k^2 = \sum_{i=1}^{N} R_{ki}^2. \tag{16}$$

The *noise factor* f_k describes how much the noise in the input data is amplified for a given operator R. It is not dimensionless, and depends on the adopted units, system parameters, etc.

So, we have at hand the formalism permitting to reconstruct the profile with any desired resolution and to study the noise properties of this reconstruction. This formalism is even more general. If $M(0)$ is needed to estimate the Fried radius, the weighting function $W = 1$ must be chosen. For isoplanatic angle calculation we need $W_j = h_j^{5/3}$. Thus, quantities of interest can be obtained from the $C(r)$ without explicit profile computation.

5.2 Numerical experiment

In our numerical simulation we suppose that atmosphere consists of 20 discrete layers at 1,2,..20 km. We simulate three turbulent layers at 5, 10 and 17 km with integrated intensities of 6, 12 and $4 \cdot 10^{-14}\ m^{-1/3}$ (the integrated seeing of such an atmosphere corresponds to $r_0 = 20$ cm at $\lambda = 500$ nm).

A detector with 2 cm pixels measures the light intensity in the pupil plane, and the normalized auto-correlation function (ACF) $C(r)$ is computed on a 2 cm grid. We leave aside the 2-D character of data and consider only a 1-D cut of the ACF - a total of 11 measurement points from 0 to 20 cm with 2 cm step. Corresponding ACF values are obtained by multiplication of the profile by the pre-computed matrix Q corresponding to the selected instrument geometry (we consider monochromatic light with $\lambda = 500$ nm). The scintillation index $\sigma_I^2 = 0.17$ for this simulation.

A gaussian noise is added to the measured covariances. We suppose that a sufficiently bright star is observed (see below), and dominant noise comes not from photon fluctuations but from the statistical noise of atmospheric speckle. The rms speckle noise $\sigma_{\rm speckle}$ at any point of the ACF can be estimated as

$$\sigma_{\rm speckle} = \sigma_I^2 (N_i N_s)^{-1/2}, \tag{17}$$

where N_i is the number of processed images and N_s is the number of spatial samples in the pupil plane, which can be estimated as the ratio of the pupil area to the area of speckle $0.355\lambda h$ [19]. With a 30 cm telescope we have roughly $N_s = 40$. [2] An integration during 500 s with frame rate of 50 images per second gives $N_i = 25000$. Thus, a noise level of $10^{-3}\sigma_I^2$ can be achieved, and this value is adopted in our simulation.

Next step would be the definition of suitable weighting functions W_{ki} and a solution of the Eq.(14) to find the corresponding restoration operators R. This is a purely numerical exercise. Eq.(14) has an ill-conditioned matrix. It means that rather different solutions R can correspond to almost identical input vectors W. In this situation it is recommended to use the so-called *singular value decomposition* (SVD) of the matrix Q [15]. Then the eigenvalues of Q that are too small (smaller than some threshold multiplied by the largest eigenvalue) are set to zero. In this way an approximate solution R is found which has one very important property: its quadratic norm is smaller than the norm of the exact solution. We have seen that the reconstruction noise is directly related to the norm of R (Eq.15). So, by playing with the threshold we can obtain a restoration operator which gives a good approximation to the desired weighting functions W while having low noise factor.

[2] There should be no confusion between the number of detector pixels 15x15=225, the number of degrees of freedom $N_s = 40$ and the number of points on the ACF in one dimension $N = 11$.

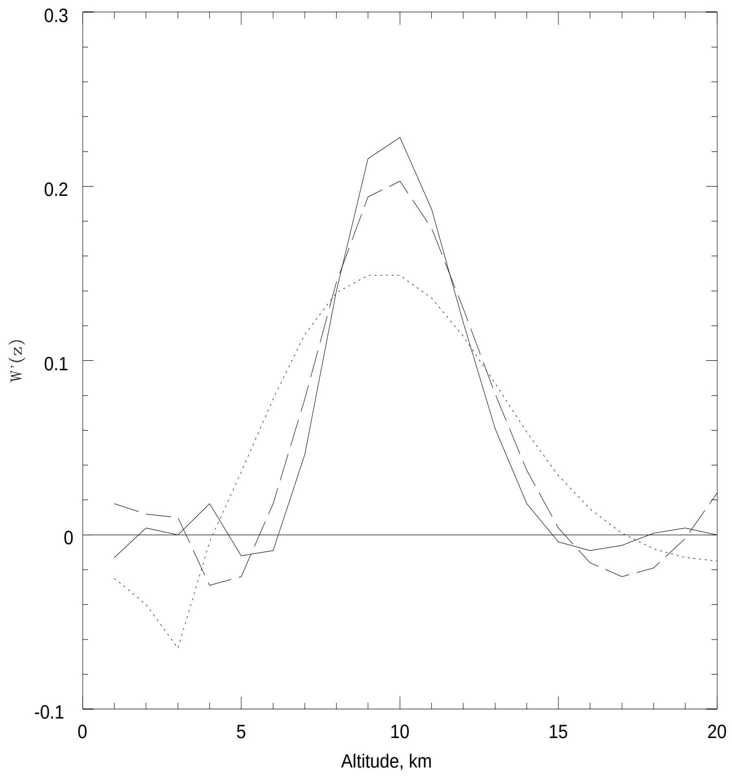

Figure 2: The resulting weighting functions $W'(z)$ obtained from the same input gaussian WF by truncating 3, 5, and 7 eigenvalues (full, dashed and dotted lines, respectively). The resolution is progressively degraded, and oscillations increase when more eigenvalues are truncated.

When the restoration operator R obtained from the SVD solution is put back into Eq.14, the resulting weighting function W' is obtained, which is not the same as the input weighting function W. The choice of the SVD threshold does not depend on the noise in the input data, it only determines how close our real weighting functions W' will be to the "ideal" weighting functions W that we supply at input. Too high thresholds produce a too smooth weighting functions, and low thresholds lead to increase of restoration noise without increase of resolution.

The shape and width of the desired weighting functions also have an important effect on the restoration noise. If we want "box-shaped" functions which fall off sharply, restoration operators are noisy, and the weighting functions calculated by SVD have oscillations. So, better results can be obtained with smooth $W(h)$. We select a set of gaussian weighting functions

$$W_k(h_j) = W_{0k} \exp[-(h_j - h_k)^2/(2\sigma_k^2)] \text{ with } \sigma_k = 0.5\text{km}\sqrt{h_k[\text{km}]}, \tag{18}$$

where a normalizing constant W_{0k} is calculated to give a unit sum of W_{kj} over all altitudes h_j. A particular choice of dispersion is not very critical, but seems to be reasonable: at low altitudes where sensitivity is bad we compensate for it by decreased relative resolution. For this reason the noise factors in the 5 to 20 km altitude range vary only by 2 times.

The influence of the SVD threshold on the width of resulting weighting functions W' is illustrated in Fig. 2 and the following Table. A gaussian $W(z)$ peaking at 10 km is given at input, and Eq.14 is solved by setting to zero more and more eigenvalues of Q, beginning with the smallest ones (N_0 is the number of truncated eigenvalues). The FWHM of the resulting $W'(z)$ is then estimated (input FWHM = 3.7 km/s), as well as the noise factors f. With increasing N_0 the condition number of the modified matrix Q goes down and FWHM increases. Also, the oscillations in the $W'(z)$ become more important. Finally, in our simulations the SVD

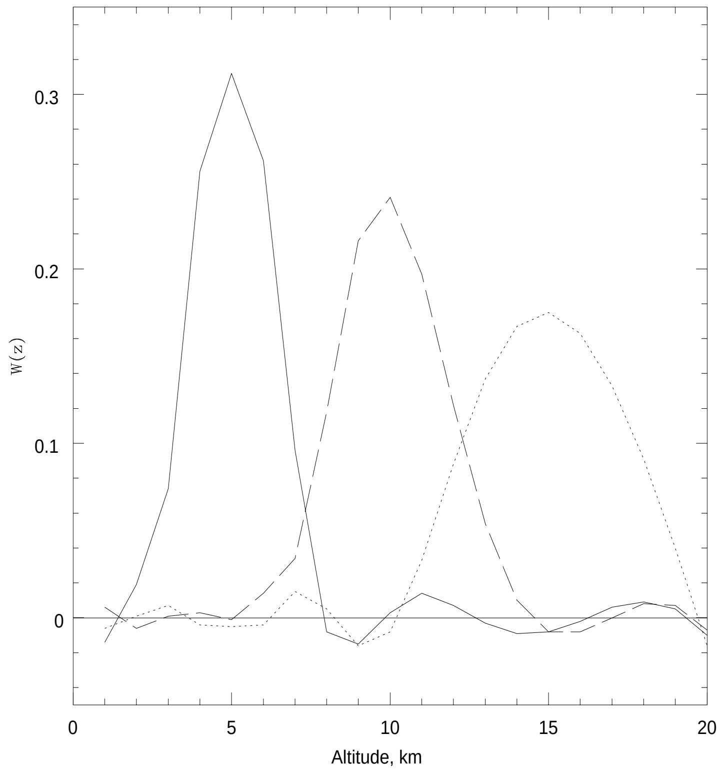

Figure 3: Three quasi-gaussian weighting functions $W'(z)$ with peak altitudes of 5, 10 and 15 km. They are obtained from input gausian functions using the SVD matrix inversion with a 10^{-3} threshold.

threshold is set to 10^{-3}, suppressing only the two smallest eigenvalues.

Number of truncated eigenvalues N_0	1	2	3	4	5	6	7
Log of condition number	3.0	2.8	2.6	2.4	2.2	2.1	1.8
FWHM of $W'(z)$, km	4.0	4.0	4.4	5.2	5.4	5.8	7.5
Noise factor f	971	965	796	477	460	395	192

After SVD solution of Eq.(14) with input weighting functions given by Eq.(18) a set of restoration operators is obtained. They have typical oscillatory behavior. For example, the restoration operator for a layer at 10 km looks like this:

i	1	2	3	4	5	6	7	8	9	10	11
R_i	95	-217	277	-235	65	-200	350	-69	-274	399	24

The three weighting functions resulting from the SVD solutions are plotted in Fig. 3 for the layers at 5, 10 and 15 km. It can be noted that they are not *exactly* gaussian, but residual oscillations seem to be at acceptable level. These oscillations result from the SVD regularization as explained above, and are controlled by the threshold parameter.

In Fig. 4 the input and reconstructed turbulence profiles are plotted. The errors of the reconstructed profile are about $2 \cdot 10^{-15} m^{-1/3}$ at 5 km and two times less at 15-20 km. To express this error in terms of C_n^2, we must divide it by the equivalent width of the weighting function, e.g. by 3.11 km at 5 km and by 4.8 km at 15 km, which leads to errors of $6 \cdot 10^{-19}$ and $2 \cdot 10^{-19}$ $m^{-2/3}$ at 5 and 15 km, respectively. The input profile corresponded to the realistic conditions in the free atmosphere, and it is reconstructed with 10% relative accuracy. It must

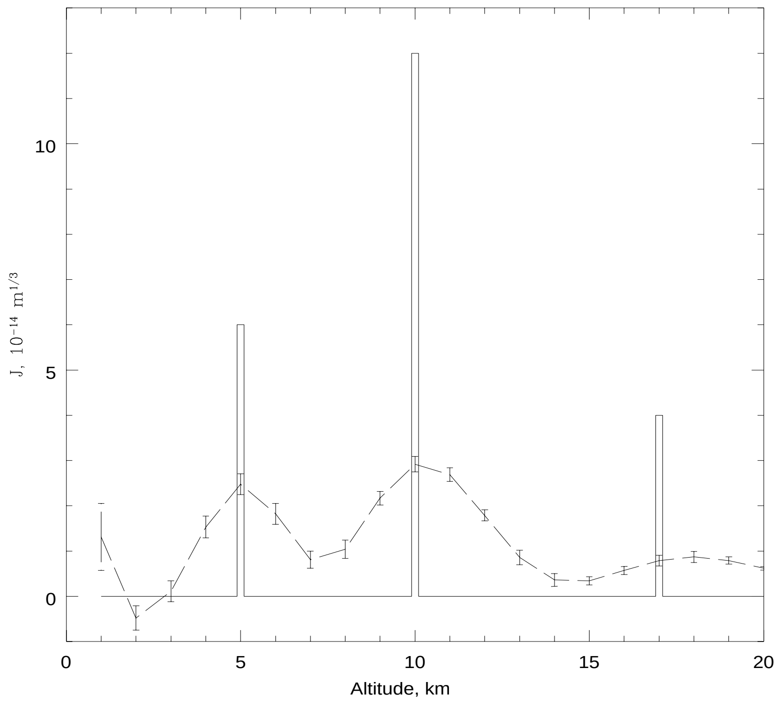

Figure 4: Input turbulence profile (full line) and its restoration with weighting functions (dashed line). Error bars correspond to the relative input ACF noise of 10^{-3} and are calculated using Eq.(16). The sum of restored profile is $22.4 \cdot 10^{-14}$ $m^{1/3}$, in good agreement with the input value of $22.0 \cdot 10^{-14}$.

be noted that the errors at adjacent altitudes are not independent.

In summary, a modest altitude resolution of $\Delta h/h = 0.4$ (at 10 km) can be achieved with acceptable noise permitting profile measurement with a 10% relative accuracy in a time of about 10 min. This requires measuring the scintillation ACF with a 10^{-3} relative accuracy, which is theoretically possible. The summary of the reconstruction procedure is given in Fig. 5.

5.3 Instrumental considerations

Major experimental problem likely to be encountered at this level of accuracy is the systematic error on the ACF. It may arise for several reasons:

- Detector defects (sensitivity variations, non-linearity, periodic noise), if not taken into account properly. The relative accuracy ACF of 10^{-3} translates into the requirement to reduce systematic errors on intensity below 10^{-2}, which seems possible.

- Finite exposure time and associated elongation of ACF in the direction of dominant wind. It may be necessary to reduce the exposure time, or to analyze the ACF only in the direction perpendicular to the wind.

- Elongation of ACF due to the chromatic refraction in the atmosphere for stars away from zenith. For example, a bandwidth of 100 nm corresponds to chromatic shift up to 1.5 cm for a star at zenith distance of 30^o (see [4] for the calculation of this shift). This effect can not be compensated, because the shift is altitude-dependent.

It is not feasible to consider these (and other) potential problems theoretically. Their importance and method of correction can be investigated on a working prototype only, and would require considerable practical experience.

A comment on source brightness and detector parameters must be made here. The classical SCIDAR studied in [19] is limited by the choice of suitable binary stars, which are not very

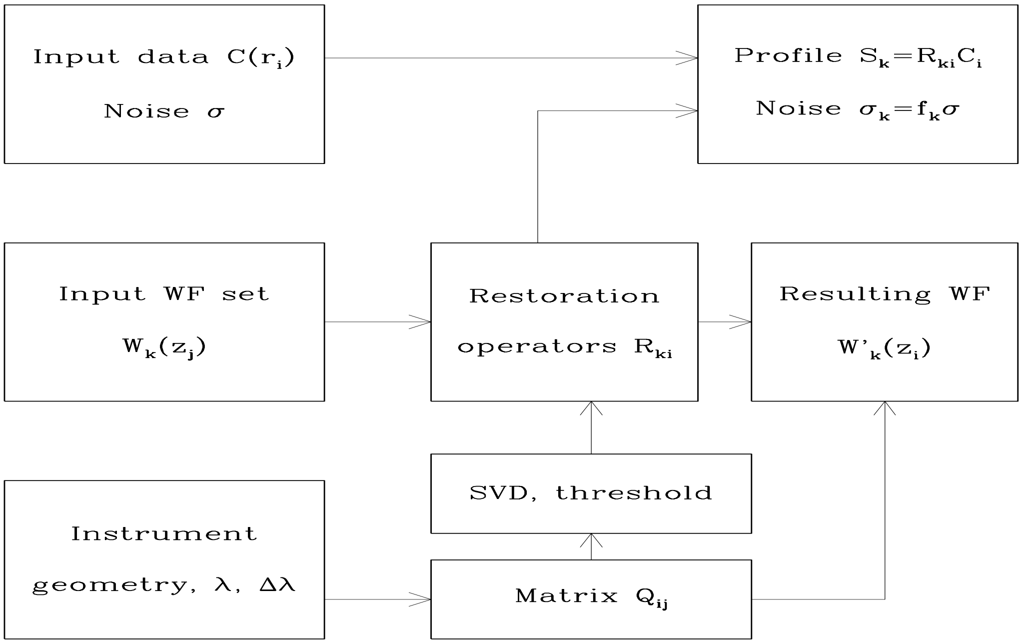

Figure 5: The schematic block diagram of the linear profile restoration with weighting functions.

bright and require a good low-noise detector. Here the situation is better, and it is clear that a 2.5^m star can always be selected as a source. Taking the CCD detector parameters from [19], we can see that such a star will produce 100 photoelectrons per pixel per 1 ms exposure. The speckle pattern is more contrasted than in SCIDAR; so, the contribution of photon noise will be equal to speckle noise for a 7.5^m star. Similarly, if detector readout noise is much less than 100 e^-, it's effect will be negligible. This is why the photon and detector noise were neglected in our preliminary analysis.

The analysis given above is on the pessimistic side because only 1-D data are considered. For 2-D data the restoration process consists in multiplication of ACF by a rotationally-symmetric function $R(r)$ (with alternating positive and negative rings). The formalism given above can be applied, but the dimension of the input data vector and matrix Q would be greater. It is not yet clear what degree of noise reduction is to be expected, because speckle noise in the ACF is correlated; with 40 degrees of freedom, compared to 11 1-D points, the gain in signal to noise must not exceed 2.

When the real data are processed, we will have to take into consideration the finite bandwidth of the light source and detector. This would imply averaging of the matrix Q over the spectral bandpass, as was done in [12, 10]. Our monochromatic simulation is suitable only to demonstrate the validity of the proposed approach.

5.4 Other methods of profile reconstruction from ACF

The problem of reconstruction of a turbulence profile from ACF is not a new one. First analytical solution was given by Peskoff in 1968 [13]. Later Jarem [8] used Tikhonov's regularization technique in profile inversion, which is equivalent to smoothing. This method was tested by

Stevens [17] on a simulated profile. From his work it is not clear how the noise was treated. [3] Anyway, all these methods are linear ones and can be implemented in a more direct way using the matrix formalism given here.

Another flavor of linear technique can be developed if turbulence profile is sought as a polynomial (or some other function set) expansion. By limiting the degree of polynomial a smoothing (or regularization) is achieved. Matrix equation which relates the unknown coefficients to the measured quantities can be written and solved (by least-squares technique if it is over-determined). For example, if r_0 is known and scintillation indices are measured at the same time with small and large apertures, we know $M(0)$, $M(5/6)$ and $M(2)$ moments of the profile, from which a quadratic polynomial can be calculated. Adding more independent data (e.g. scintillation index measured in a generalized mode or ACF) may increase the degree of polynomial and make this approach an interesting possibility.

The family of *non-linear* restoration techniques is large. They can take advantage of additional *a priori* information, like non-negativity of the profile. For example, the maximum entropy method is used routinely by the Vernin group in SCIDAR data processing. As suggested by H. Lanteri (private communication), the so-called *Iterative Image Space Reconstruction* (ISRA) [18] is well-suited for profile reconstruction. It was shown [14] that ISRA iterations converge to a solution which is the best least-squares fit to the input data with positivity constraint. By limiting the number of iterations, a regularization is achieved. Whatever the non-linear method used, its noise analysis is not so simple as in the linear case, and probably can be done only via extensive numerical simulation.

A possible non-linear method can be envisaged which uses the *a priori* knowledge that realistic turbulence is usually concentrated in few thin layers. Thus we can look for a solution which would represent the true profile by few delta-functions corresponding to the layers. In this way a better idea on the altitude of layers can be obtained (as compared to the weighting-functions reconstruction). It is not yet clear how to implement this idea. One possibility is the *simulated annealing* [15]. A less heavy method can start from the smooth initial reconstruction and then iteratively improve layer altitudes and strengths by non-linear least-squares procedure, which at the same time would provide formal errors of these parameters. Some analogy between this *layer decomposition* method and the CLEAN image reconstruction method can be noted.

Real data are needed to investigate and compare different profile reconstruction methods. Only after considerable experience can we hope to identify the best reconstruction method and to assess its performance.

The SCIDAR is a good but expensive profiler which needs large telescope. Now, if we are ready to accept the lower altitude resolution of single-star profilers, it may be advantageous to use a close (1-2 arcsec) binary star instead of a single star. The ACF in this case can still be measured with a small (30 cm) telescope, but the matrix Q would be better conditioned, which would improve the performance. It remains to be seen how many suitable bright binaries exist, but they must be more numerous than SCIDAR sources because it is easier to find a close binary than a wider one [19]. The hardware for single and binary star observations is the same. So, a hybrid strategy can be adopted: use double star when available and switch to single star otherwise.

[3] From this thesis we may guess that single-star profiler based on ACF processing was previewed at Rome Air Development Center in 1985. Has it ever been built and tested?

6 Alternative single-star profilers

In this section the alternative approaches to remote profile measurement are briefly reviewed.

6.1 Atmospheric dispersion profiler

Every star can be viewed as a close binary when observed away from zenith at different wavelength, because the chromatic atmospheric refraction bends rays of different colors by different angles. Thus, speckle patterns in two colors produced by a high-altitude layer at telescope pupil will be shifted relative to each other, which can be exploited to obtain turbulence profile [4]. To our knowledge, no data were produced routinely by this technique. The altitude resolution must be poor ($\Delta h/h \approx 1$) because by the nature of chromatic refraction the shift is small. Shift can be increased by going to large zenith angles, but only in conditions of weak turbulence, because for $\gamma > 60^o$ scintillation begins to saturate and theory is no longer applicable.

6.2 Using the spatio-temporal correlation

In [3] it was suggested to measure the profile by spatio-temporal correlation of speckle (i.e. correlation between 2 delayed frames). Peaks corresponding to layers with different velocities are displaced by different amounts from the coordinate origin, and so can be separated. The displacement can be kept small if small time lags (few ms) are used, to fit into 30-cm telescope aperture. This method works well when there are only few layers and their altitudes and velocities are known from independent meteo soundings. If no meteo data are available, layer altitudes are found from peak widths. But things get much worse when peaks are superimposed. The problem of getting simultaneous wind and turbulence profile in a general case was not yet solved even for the classical SCIDAR (J. Vernin, private communication). So, this method must be kept under consideration and needs further theoretical development.

6.3 Generalized profiler

Another interesting possibility is to use the generalized scidar principle [6, 1]. Suppose that the scintillation index is measured with a small aperture focused on different virtual altitudes h_0. The weighting function is proportional to $|h - h_0|^{5/6}$. Thus scintillation index is completely insensitive to turbulence at altitude h_0. Combining scintillation indices measured at different h_0 and solving the matrix equation, we can obtain the profile.

Limitation of this technique is primarily caused by scintillation saturation: for large values of h_0 the turbulent layer near ground will produce a too strong scintillation. Let us assume that ground layer alone gives a $1''$ seeing ($r_0 = 10$ cm at 500 nm), as typical for many good sites. It corresponds to the integral $J = 6.80 \cdot 10^{-13} m^{1/3}$. A scintillation index of 0.3 (saturation limit) is obtained for $h_0 = 5.3$ km. The generalized scidar never uses $h_0 > 4$ km for this reason. For weak turbulence the altitude limit is increased, e.g. $h_0 < 15$ km for $r_0 = 20$ cm. So, in the general case the defocusing limit will not be large enough to probe the whole atmosphere from 0 to 20 km. Nevertheless, with this approach a good profile in the lowest few kilometers can be obtained.

The method was modeled numerically. We suppose that scintillation index is measured with a small aperture for the range of h_0 from 0 to 7.5 km with 0.5 km step, thus giving $N = 16$ data points $C_i = \sigma_I^2(h_{0i})$, $i = 1, ..N$. The wavelength $\lambda = 500$ nm is assumed. Relation between C_i

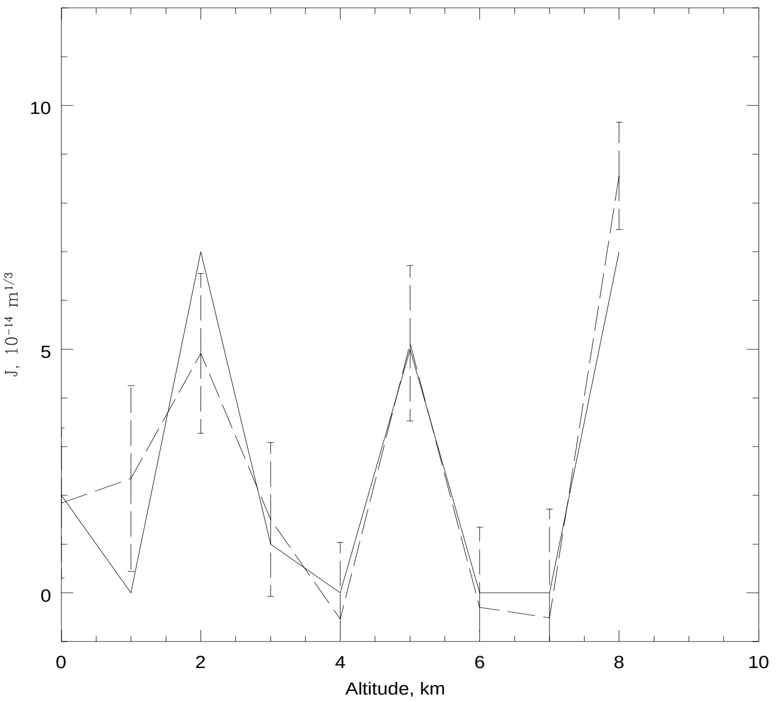

Figure 6: Input turbulence profile (full line) and its restoration with generalized profiler (dashed line) for virtual altitude range from 0 to 7.5 km with 0.5 km step. Error bars correspond to the relative input noise of 0.02. Last point at $h = 8$ km represents the sum of all upper layers. The sum of restored values is $22.9 \cdot 10^{-14}$ $m^{1/3}$, to compare with $22.0 \cdot 10^{-14}$ for input profile.

and $C_n^2(h)$ is given by the formula (8.5) of Roddier [16]. When M discrete layers with 1 km step are taken, each having the integrated turbulence J_j, this relation takes the form

$$C_i = \sum_{j=1}^{M} U_{ij} J_j, \tag{19}$$

$$U_{ij} = 19.12 \lambda^{-7/6} |h_j - h_{0i}|^{5/6}. \tag{20}$$

If Eq. (19) is solved directly, it becomes evident that for altitudes higher than h_{0max} no meaningful result is obtained, as expected (the weights with which the upper layers are combined to produce σ_I^2 are not sufficiently different). We limited the number of unknowns to the 8 layers corresponding to h_j from 0 to 7 km. The combined effect of upper layers is taken into account by averaging all columns U_{ij} over j for $j > 8$ and adding the integrated turbulence in the upper layers as one additional 9-th unknown. Now the problem becomes well-behaved (condition number of the modified matrix U is 61) and direct matrix inversion is feasible. We tried to add data at negative h_0 and saw that they do not improve the quality of the solution.

Let us estimate the noise on C_i. If all altitudes h_{0i} are scanned sequentially for 300 s, the integration time T is about 20 s per point. With signal time constant $\tau = 10^{-3}$ s relative statistical error of dispersion measurement would be $(T/\tau)^{-0.5} = 7 \cdot 10^{-3}$ (this is only a crude estimate). In our numerical model we have taken the relative noise of 0.02, which is perhaps more realistic because τ for scintillations is around a few hundred Hz.

In Fig. 6 the input and restored profiles are compared. For several simulated data sets we noted that the restored value at 7 km is negative, but it's sum with the last "upper-layer" value (plotted at 8 km) always gives a fair estimate of integrated turbulence strength above 7 km, despite the fact that its treatment in our matrix equation was very primitive. At lower altitudes the error bars are about $1.5 \cdot 10^{-14}\ m^{1/3}$. They are directly proportional to the input data noise, as in any linear method.

Results of our first modeling look encouraging. The generalized profiler may prove to be a good method for the characterization of orographic turbulence around observatory, including the lowest layers. More studies are needed to find the limits on altitude resolution, which can be perhaps much better than 1 km.

The generalized profiler can be conceived as a small telescope equipped with a photomultiplier light detector and a mechanical device to scan repeatedly the selected range of virtual altitudes. A single optical fiber whose entrance is moved back and forth along the optical axis can play a role of input aperture. If a 10 μ fiber core is projected into 1 cm entrance aperture, the magnification factor is $G = 1000$. The scanning range in the exit pupil is equal to h_0/G^2, or 7 mm for $h_{0max} = 7$ km.

The size of telescope aperture is determined by two effects. First, the generalized scidar theory is valid only for infinite aperture; it means that edge effects are to be avoided. The Fresnel radius for $h_0 = 7$ km is about 6 cm, and aperture size must be no less than 6+6+1=13 cm (probably much more: a special study is needed to find how close to aperture edge the diffraction begins to be troublesome for this instrument). The second effect is related to source motion due to guiding errors. The image of exit pupil is stable, but the defocused image does move. It's displacement d (in the input aperture scale) is simply $d = \alpha h_0$, where α is the source angular displacement. Putting a rather severe requirement $|\alpha| < 1''$, we have $|d| < 34$ mm, so aperture size must be increased by another 7 cm. On the total, we need a clear (i.e. without central obscuration) aperture of at least 20 cm size. The telescope must be of reasonably good optical quality and with good guiding. The prototype device can be tested on existing telescopes of, say, 60 cm class, using the off-axis portion of aperture which is clear from central obscuration and spiders.

7 Conclusions

It appears possible to obtain a low-resolution C_n^2 altitude profile from observations of a single bright star with a 2-D fast detector. Our preliminary study shows the feasibility of this modern scintillometer. Alternative profilers considered in Sect. 6 need more investigation before their limitations are fully understood.

A large amount of work is still to be done before a single-star profiler based on modern technology becomes available. It includes mathematical development, numerical modeling, device prototyping and experiments. All these directions are important and must be pursued simultaneously. Only after fruitful interaction between experiment and theory the best available data processing method will be identified and exact hardware specifications will be established.

The prototype instrument for the study of the proposed methods is similar to SCIDAR [19]. Its major component is a fast detector with low readout noise and small number of pixels. Noise specifications, however, are less stringent than for a double-star SCIDAR, because brighter stars are available. A TV-readout rate CCD camera with a fast shutter may be an attractive possibility. Experiments can be conducted on existing telescopes.

References

[1] Avila R., Vernin J., Masciadri E. Whole atmosphere profiling with a Generalized Scidar.

Appl. Opt., 1997, V. 36, P. 7898-7905.

[2] Azouit M., Vernin J. Remote investigation of tropospheric turbulence by two-dimensional analysis of stellar scintillation. J. Opt. Soc. Amer., 1980, V. 37, P.1550-1557.

[3] Caccia J.L., Azouit M., Vernin J. Wind and C_N^2 profiling by single-star scintillation analysis. Appl. Opt., 1987, V. 26 P. 1288-1294.

[4] Caccia J.L., Vernin J., Azouit M. Structure function C_n^2 profiling by two-color stellar scintillation with atmospheric dispersion. Appl. Opt., 1988, V. 27 P. 2229-2235.

[5] Eaton F.D., Peterson W.A., Hines J.R., Fernandez G. Isoplanatic angle direct measurements and associated atmospheric conditions. Appl. Opt., 1985, V. 24, P. 3264-3273.

[6] Fuchs A., Tallon M., Vernin J. Focusing on a turbulent layer: Principle of the "Generalized - Scidar". Applied Optics, 1997, submitted.

[7] Fried D.L. Anisoplanatism in adaptive optics. JOSA, 1982, V. 72, P. 52-61.

[8] Jarem J. Remote sensing of Structure Constant Profiles using Tikhonov's Regularization Fourier Integral Method. Appl. Opt., 1984, V. 23, P. 2614-2619.

[9] Klückers V.A., Wooder N.J., Nicholls T.W., Adcock M.J., Munro I., Dainty J.C. Profiling of atmospheric turbulence strength and velocity using a generalized SCIDAR technique. Astron. Astrophys. Suppl. Ser., 1998, submitted.

[10] Krause-Polstorf J., Murphy E.A., Walters D.L. Instrument comparison: corrected scintillometer versus isoplanometer. Appl. Opt., 1993, V. 32, P. 4051-4057.

[11] Loos G., Hogge C. Turbulence of the upper atmosphere and isoplanatism, Appl. Opt., 1979, V. 18, P. 2654–2661.

[12] Ochs G.R., Ting-i Wang, Lawrence R.S., Clifford S.F. Refractive-turbulence profiles measured by one-dimensional spatial filtering of scintillations. Appl. Opt., 1976, V. 15, P. 2504-2510.

[13] Peskoff A. Theory of remote sensing of clear-air turbulence profiles. JOSA, 1968, V. 58, P. 1032-1040.

[14] De Pierro A.R. On the relation between the ISRA and the EM Algorithm for Positron Emission Tomography. IEEE Trans. on Medical Imaging, 1993, V. 12, P. 328-333.

[15] Press W.H., Flannery B.P., Teukolsky S.A., Vetterling W.T. Numerical Recipes in C: The Art of Scientific Computing. Cambridge University Press, 1988.

[16] Roddier F. The effects of atmospheric turbulence in optical astronomy. Progress in Optics, 1981, V. 19, P.281.

[17] Stevens K.B. Remote measurements of the atmospheric isoplanatic angle and determination of refractive turbulence profiles by direct inversion of the scintillation amplitude covariance function with Tikhonov regularization. Ph.D. dissertation, Naval Postgraduate School, Monterey, Calif., 1985.

[18] Titterington D.M. On the Iterative Image Space Reconstruction Algorithm for ECT. IEEE Trans. on Medical Imaging, 1987, V. MI-6, P. 52-56.

[19] Tokovinin A.A. Study of the SCIDAR concept for adaptive optics applications. ESO Doc. VLT-TRE-UNI-17416-003, March 1997.

[20] Tokovinin A.A. A new method to measure the atmospheric seeing. Astron. Letters, 1998, submitted.

[21] Vernin J., Azouit M. Traitement d'image adapté au speckle atmosphérique. I. Formation du speckle en atmosphère turbulente. Propriétés statistiques. J.Optics (Paris), 1983, V. 14, P.5-9.

[22] Vernin J., Azouit M. Traitement d'image adapté au speckle atmosphérique. II. Analyse multidimensionelle appliquée au diagnostic à distance de la turbulence. J.Optics (Paris), 1983, V. 14, P. 131-142.